

Traffic Scene Parsing through the TSP6K Dataset

Peng-Tao Jiang¹ Yuqi Yang² Yang Cao³ Qibin Hou^{2*} Ming-Ming Cheng² Chunhua Shen¹
¹CAD&CG, Zhejiang University ²TMCC, CS, Nankai University ³ HKUST

Abstract

Traffic scene parsing is one of the most important tasks to achieve intelligent cities. So far, little effort has been spent on constructing datasets specifically for the task of traffic scene parsing. To fill this gap, here we introduce the TSP6K dataset, containing 6,000 urban traffic images and spanning hundreds of street scenes under various weather conditions. In contrast to most previous traffic scene datasets collected from a driving platform, the images in our dataset are from the shooting platform high-hanging on the street. Such traffic images can capture more crowded street scenes with several times more traffic participants than the driving scenes. Each image in the TSP6K dataset is provided with high-quality pixel-level and instance-level annotations. We perform a detailed analysis for the dataset and comprehensively evaluate the state-of-the-art scene parsing methods. Considering the vast difference in instance sizes, we propose a detail refining decoder, which recovers the details of different semantic regions in traffic scenes. Experiments have shown its effectiveness in parsing high-hanging traffic scenes. Code and dataset will be made publicly available.

1. Introduction

As a classic and important computer vision task, the scene parsing task aims to segment the semantic objects and stuff from the given images. Nowadays, the emergence of large-scale scene understanding datasets, such as ADE20K [61] and COCO-Stuff [2], has greatly promoted the development of scene parsing algorithms [34, 58]. Many application scenarios, such as robot navigation [13, 26] and medical diagnosis [37], benefit from these scene parsing algorithms [30, 34].

As an important case of scene parsing, traffic scene parsing focuses on understanding urban street scenes, where the most frequently appeared instances are humans and vehicles. To date, there are already a few large-scale publicly available street scene datasets, such as KITTI [18], Cityscapes [12], and BDD100K [48]. A characteristic of

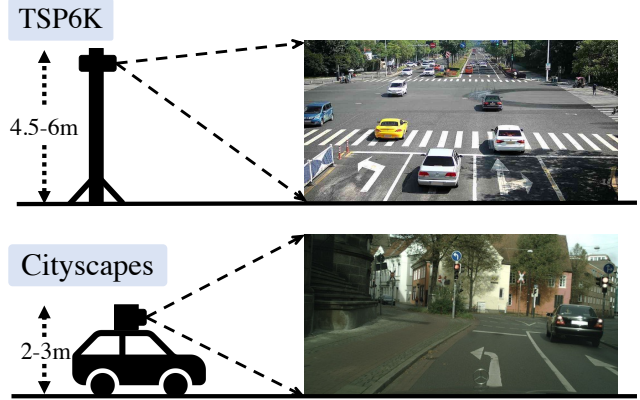


Figure 1. Comparison of the ways to capture scenes between Cityscapes [12] and our TSP6K. Cityscapes collects the traffic images captured from the driving platform, such as a driving car. In contrast, the TSP6K dataset collects traffic images from the urban road high-hanging platform, which captures more crowded scenes with a broader view.

these datasets is that they are mostly collected from a driving platform, such as a driving car, as shown in Fig. 1 and hence are more suitable for the autonomous driving scenario. Benefiting from these finely-annotated datasets, the segmentation performance of the recent scene parsing approaches [8, 21, 29, 39, 54, 62] is also considerably improved.

The images from the aforementioned datasets are collected from driving vehicles. However, little attention has been moved to the high-hanging traffic scenes. This kind of traffic scenes is captured by the shooting platform high-hanging on the street¹, which can offer a rich vein of information on traffic flow [27, 35]. We summarize the differences between the high-hanging and the driving traffic scenes as follows. **(i) Broader view:** The urban road shooting platform hangs at a high location (4.5-6 meters) on the street, which is more than twice higher than the driving platform. The high-hanging platform sees more street content than the driving one, as shown in Fig. 1, especially at the crossing. This makes the collected images from the high-hanging platform more challenging than ones from existing

*Qibin Hou is the corresponding author.

¹In the following, we call such kind of shooting platform as high-hanging platform.

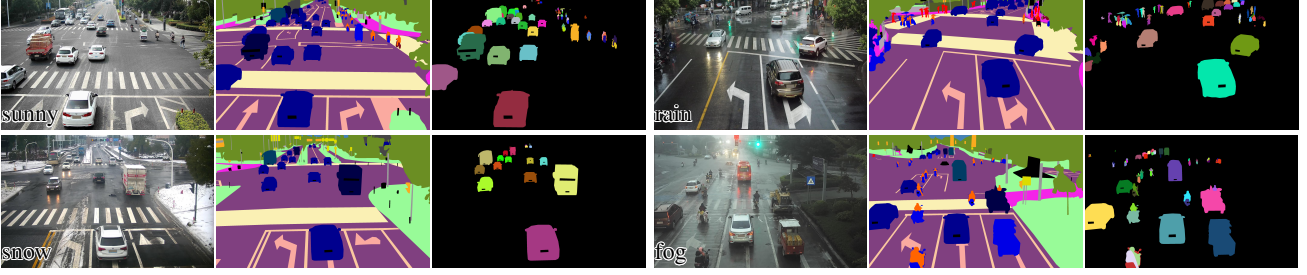


Figure 2. Examples are randomly picked from the TSP6K dataset. Each image is associated with its corresponding semantic label and instance label. We have masked the vehicle plates for privacy protection. More examples can be found in the supplemental material.

datasets. **(ii) Road indications:** High-hanging scenes provide more important categories that only occasionally appear in the driving scenes, such as the zebra crossing and driving indicators. These road indications are important for analyzing traffic conditions.

To facilitate the research on the high-hanging traffic scenes, we collect many traffic images from the urban road shooting platform. To keep the diversity of our dataset, we collect high-hanging images from hundreds of traffic scenes under different weather conditions and times in a day. In total, we collect 6,000 traffic images and ask annotators to finely annotate them with semantic-level and instance-level labels. In Fig. 2, we have shown four traffic images under different weather conditions and the corresponding semantic-level and instance-level labels.

Based on the proposed TSP6K dataset, we evaluate many classic scene parsing approaches on the proposed benchmark and summarize several valuable tips for high-hanging scene parsing. Besides, we propose a detail refining decoder for high-hanging scene parsing. The detail refining decoder utilizes the encoder-decoder structure and refines the high-resolution features by a region refining module. The region refining module utilizes the self-attention mechanism and computes the attention between the pixels and each region token. The attention is further used to refine the pixel relationships in different semantic regions. The proposed method has achieved 75.4% mIoU score and 58.1% iIoU score on the TSP6K validation set. To verify the effectiveness of each component in the detail refining decoder, we also conduct a series of ablation experiments.

In summary, the contributions of this paper are summarized as follows:

- We propose a new dataset, termed TSP6K, which collects traffic images spanning various scenes from the urban road high-hanging platform. We provide pixel-level annotations of fine semantic labels and instance labels.
- Based on the TSP6K dataset, we evaluate many recent state-of-the-art methods and analyze their performance. We summarize a few tips for benefiting the high-hanging street scene parsing.

- To improve street scene parsing, we propose a detail-refining decoder, which learns several region tokens and compute the attention maps between the tokens and the high-resolution features. The attention is further used to refine the details of different semantic regions. Experiments validate the effectiveness of the proposed decoder.

2. Related Work

2.1. Scene Parsing Datasets

Scene parsing datasets with full pixel-wise annotations are utilized for training and evaluating the scene parsing algorithms. As an early one, the PASCAL VOC dataset [16] was proposed in a challenge, which aims to parse the objects of 20 carefully selected classes in each image. Later, the community proposed more complex datasets with much more classes, such as COCO [32], ADE20K [61]. The scenes in the above datasets span a wide range. Besides, different from them, some datasets focus on particular scenes, such as the traffic scenes. There exist many traffic scene parsing datasets [24, 36, 51, 52], such as KITTI [18], Cityscapes [12], and BDD100K [48]. These traffic parsing datasets annotate the most frequent classes in the traffic scenes, such as traffic sign, rider, and *etc.* With the help of these finely-annotated traffic datasets, the approaches based on the neural networks achieved great success in parsing the traffic scenes. Furthermore, some datasets [14, 38] focus on the night driving scenes.

Despite the success of the above datasets, we find the traffic scenes in these datasets all from the driving platform. The models trained on these datasets often behave not well on parsing the traffic scenes obtained from the urban road high-hanging platform. The high-hanging platform usually has a larger view than the driving platform, which captures much more crowded scenes. Our dataset that focuses on high-hanging scenes is a supplement to current traffic datasets.

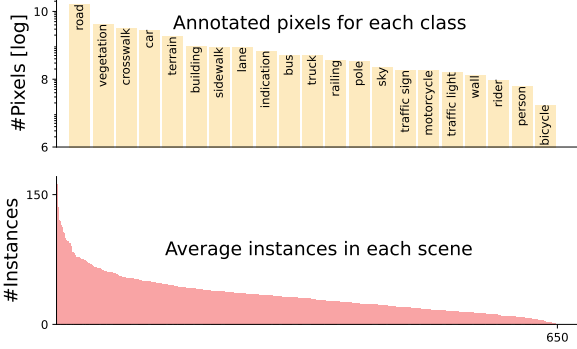


Figure 3. Class and scene information of the TSP6K dataset.

2.2. Scene Parsing Approaches

Convolutional neural networks have facilitated the development of scene parsing approaches. Long *et al.* [34] first proposed a fully convolutional network (FCN) that generates dense predictions for scene parsing. Later, some approaches, such as the popular DeepLab [4, 5] and PSP-Net [58], have benefited from large receptive fields and multi-scale features, improving the performance by a large margin. Besides, there are also some approaches, including SegNet and DeepLabv3+ *et al.* [1, 7, 8, 30], utilizing the encoder-decoder structure to refine the low-resolution coarse predictions with the details of the high-resolution features.

Recently, researchers found the attention mechanism modeling long-range dependencies among pixels can improve the scene parsing networks. Some approaches, such as PSANet [59] and OCNet [50], directly apply the attention mechanism on the backbone features to model long-range context dependencies, which highly improves the segmentation performance. However, using self-attention brings heavy computing costs. This motivated some researchers to attempt to reduce self-attention by introducing strip pooling or criss-cross attention [23, 25].

With the successful introduction of Transformers into image recognition [15], researchers have attempted to apply Transformers to the segmentation task [9, 10, 39, 45, 60]. A typical example should be SegFormer [45], which greatly improves previous CNN-based models by a large margin. Furthermore, another research line [43, 46, 47, 55, 57] explores real-time scene parsing algorithms, which gives attention to both effectiveness and efficiency.

3. Dataset and Analysis

3.1. Data Collection

One significant aspect of researching the high-hanging traffic scenes is data. Once we construct a dataset for the high-hanging traffic scenes, the community researchers can develop new algorithms based on the novel data characteris-

tics. To facilitate the research, we collect a large number of traffic images from the high-hanging shooting platform. To ensure the generalization of the scene parsing algorithms, we collect the traffic images from more than 600 scenes. As the crossing and pedestrian crossing are an essential part of traffic scenes, where congestion and accidents often occur, we keep a majority of the traffic scenes containing the crossing. Besides, considering the weather diversity, we select the traffic images under various weather conditions. As a result, we finally select 6,000 traffic images.

3.2. Data Annotation

After collecting data, we start to annotate the traffic images. The complete annotated classes are shown at the top of Fig. 3. Specifically, we annotate 21 classes, where most of the classes are the same as the class definition in Cityscapes [12]. We remove the unseen class ‘train’ in our dataset and add three new classes. As the indications on the road are vital for understanding the high-hanging traffic scenes, we ask the annotators to label three indication classes, namely crosswalks, driving indications, and lanes. Similar to the annotation policy of Cityscapes [12], the traffic images are also annotated from back to front. To keep the quality of the labels, the annotators are asked to double-check the accuracy of the labels.

3.3. Data Split

The dataset is divided into three splits for training, validation, and test according to the ratio of 5:2:3. Images collected from different scenes are randomly split into different sets. In total, there are 2,999, 1,207, and 1,794 images for the train, validation, and test sets, respectively.

3.4. Data Analysis

The proposed dataset possesses complicated traffic scenarios. We compare the TSP6K dataset with previous traffic datasets regarding the scene type, instance density, scale invariance of instances, weather diversity, and spatial resolution. In Tab. 1 and Tab. 2, we have listed the comparison among different traffic datasets. The characteristics of our TSP6K datasets can be summarized as follows:

High-hanging scenes: To the best of our knowledge, all previous popular traffic datasets focus on the driving scenes. The images of these datasets are collected from the driving platform. Different from them, we address the complicated traffic scenes captured from the urban road high-hanging platform. Thus, our dataset is more useful for traffic flow analysis.

High instance density: One of the most important characteristics is that TSP6K has many traffic instances (*i.e.*, traffic participants), including humans and vehicles. Since the majority of the traffic scenes are shot at the crossing, the

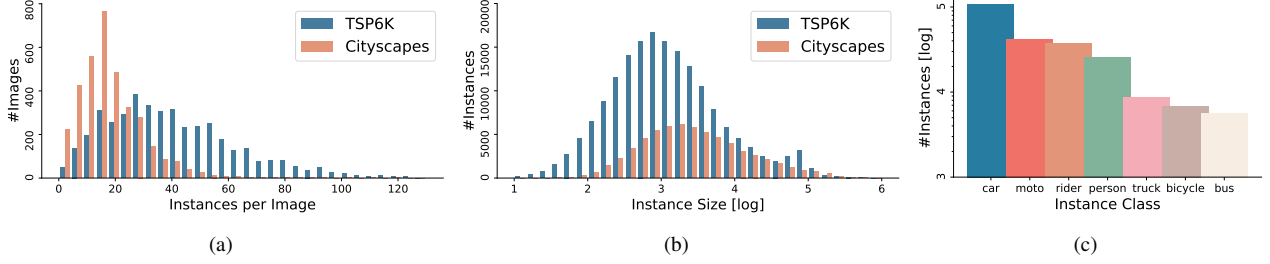


Figure 4. Data analysis of the TSP6K dataset. (a) The distribution of the number of instances in each image. (b) The distribution of the instance sizes. (c) The number of instances for each category.

Table 1. Comparison among different traffic scene parsing datasets. **Avg TP** denotes the number of the average traffic participants in each image. **TP > 50** denotes the number of images that contains more than 50 traffic participants. As the instance labels of the test sets in other datasets are not available, we all count the traffic participants in the train and validation sets. We can see that TSP6K dataset contains much more traffic images containing more than 50 traffic participants when compared with other datasets.

Type	Datasets	Class	Weather	Visibility	Image Resolution	Avg TP	TP > 50	TP > 75	TP > 100
	KITTI [18]	19	Good	High	1,241×375	4.9	0	0	0
	Cityscapes [12]	19	Good	High	2,048×1,024	18.8	54	10	4
	Mapillary [36]	65	Diverse	Low & High	3,436×2,486	12.3	102	15	3
	BDD100K [48]	40	Good	Low & High	1,280×720	12.8	5	0	0
High-Hanging	TSP6K (ours)	21	Diverse	Low & High	2,942×1,989	42.0	1,227	367	73

Table 2. Statistics of traffic participants in traffic images.

Datasets	#Humans [10 ³]	#Vehicles [10 ³]	#H./images	#V./images
KITTI [18]	6.1	30.3	0.8	4.1
Cityscapes [12]	24.4	41.0	7.0	11.8
TSP6K (ours)	64.0	188.2	10.7	31.3

instance density on the road is much larger than the driving scenes. As shown in Tab. 2, there are 10.7 humans and 31.3 vehicles in each traffic image on average. In Fig. 4(a), it can be seen that the driving datasets have few images containing more than 50 instances. In contrast, our TSP6K dataset even has a large number of images containing more than 50 instances, occupying about 30% of the images in the training and validation sets. Besides, Fig. 3 shows the number of average instances per image in each scene.

Large scale invariance of instance: For the high-hanging scenes, the scale difference of the instances in the front and end is very large, as shown in Fig. 4(b). TSP6K contains more small traffic instances than Cityscapes, which is more crowded. The high-hanging platform usually has a much broader view than the driving platform. Thus, it can capture much more content in the distance. The high scale invariance shows real traffic scenarios.

Weather diversity: In contrast to KITTI [18], Cityscapes [12], and BDD100K [48] that mainly collect traffic images with good weather conditions, we collect the traffic images

under different weather conditions, as shown in Tab. 1. The weather conditions can be mainly divided into four groups: sunny&cloudy day, rain, fog, and snow. In total, the proportions of the sunny&cloudy day, rain, fog, and snow are 60%, 22%, 8%, and 10%, respectively. The different weather conditions guarantee the generalization of the segmentation models. Besides, our dataset also considers the visibility of the traffic images. The visibility of the traffic images is limited under terrible illumination and weather conditions. In our dataset, the ratios of the low visibility and the high visibility are 15.8% and 84.2%, respectively.

High resolution: The mean spatial resolution of the captured images is 2942×1989 , which is much larger than KITTI, Cityscapes and BDD100K. The high-resolution images also ensure the clearness of the street contents, especially the small traffic participants.

4. Scene Parsing Benchmark

The scene parsing benchmark aims to evaluate the performance of previous popular scene parsing methods. We run all the scene parsing methods based on a popular codebase, mmsegmentation [11]. All the models are trained for 160000 iterations on a node with 8 NVIDIA A100 GPUs. More training settings can be found in the supplemental material. We utilize the mIoU [34] metric to evaluate the performance of the scene parsing methods. As mentioned in [12], the mIoU metric is biased to the object instances with large sizes. However, the high-hanging traffic scene is full of small traffic participants. To better evaluate the in-

Table 3. Evaluation results of previous scene parsing approaches on the TSP6K validation and test sets.

Methods	Publication	Backbone	Parameters	GFlops	Validation		Test	
					mIoU (%)	iIoU (%)	mIoU (%)	iIoU (%)
FCN [34]	CVPR'15	R50	49.5M	454.1	71.5	55.2	72.5	55.1
PSPNet [58]	CVPR'16	R50	49.0M	409.8	71.7	54.8	72.6	54.8
DeepLabv3 [6]	ArXiv'17	R50	68.1M	619.3	72.4	55.0	73.3	55.0
UperNet [44]	ECCV'18	R50	66.4M	541.0	72.4	55.2	73.1	55.0
DeepLabv3+ [7]	ECCV'18	R50	43.6M	404.8	73.1	56.1	73.9	56.3
PSANet [59]	ECCV'18	R50	59.1M	459.2	71.3	54.5	72.6	54.8
EMANet [28]	ICCV'19	R50	42.1M	386.8	72.0	55.5	72.9	55.5
EncNet [53]	CVPR'18	R50	35.9M	323.3	71.4	54.8	72.7	55.0
DANet [17]	CVPR'19	R50	49.9M	457.3	72.3	56.0	73.1	56.1
CCNet [25]	ICCV'19	R50	49.8M	460.2	72.0	55.3	73.1	55.3
KNet-UperNet [56]	NeurIPS'21	R50	62.2M	417.4	72.6	56.8	73.7	56.5
OCRNet [49]	ECCV'20	HR-w18	12.1M	215.3	73.2	55.3	73.7	55.1
SETR [60]	CVPR'21	ViT-Large	310.7M	478.3	70.5	44.9	70.7	45.0
SegFormer [45]	NeurIPS'21	MIT-B2	24.7M	72.0	72.9	54.6	73.8	54.9
SegFormer [45]	NeurIPS'21	MIT-B5	82.0M	120.8	74.5	56.7	74.8	56.7
Swin-UperNet [33]	ICCV'21	Swin-Base	121.3M	1184.6	74.9	57.4	75.6	57.2
SegNeXt [20]	NeurIPS'22	MSCAN-Base	27.6M	80.2	74.6	57.3	75.4	57.2
SegNeXt [20]	NeurIPS'22	MSCAN-Large	48.9M	258.6	74.8	57.7	75.6	57.6
SegNeXt + DRD	–	MSCAN-Base	46.1M	361.1	75.4	58.1	75.7	57.9
SegNeXt + DRD	–	MSCAN-Large	117.4M	1136.4	76.1	59.0	76.5	58.7

stances of the traffic participants, we utilize the iIoU metric over all classes containing instances, following [12].

Although the instance segmentation labels are also provided, the main purpose of this paper is the high-hanging scene parsing. We have also evaluated several classic instance segmentation methods. The evaluated results can be found in the supplemental material.

4.1. Performance Analysis

The evaluating results of different methods can be found in Tab. 3. The scene parsing methods can be roughly divided into four groups, methods using pyramid feature fusion, methods using encoder-decoder structure, methods using self-attention mechanism, and methods based on transformer structures.

Pyramid feature fusion is a very useful strategy in scene parsing. Among the evaluated methods, PSPNet [58], UperNet [44], DeepLabv3 [6], and DeepLabv3+ [7] all utilize multi-scale features. PSPNet and DeepLabv3 purely utilize the multi-scale features. (Here, FCN [34] only utilizes the last output backbone features.) It can be seen that purely using the multi-scale features brings few gains to the segmentation networks on parsing the high-hanging scenes, when comparing PSPNet to FCN. We analyze that TSP6K contains a large number of small objects, such as bicycles, and riders. The extremely downsampled features in the pyramid module may be harmful to parsing such kinds of objects, where the iIoU score also decreases when comparing PSPNet or DeepLabv3 to FCN.

Encoder-decoder structure utilizes the high-resolution low-level features to refine the details of segmentation maps. UperNet [44] and DeepLabv3+ [7] apply the encoder-decoder structure to the segmentation network. Compared with DeepLabv3 [6], DeepLabv3+ [7] utilizes the high-resolution features can further improve the segmentation results by more than 0.6% mIoU score and 1% iIoU score on both two sets. We observe that the encoder-decoder structure is very useful for small object segmentation, where the iIoU score is improved by a large margin.

Self-attention mechanism is widely used in scene parsing methods, which models the long-range pixel dependence based on the backbone features to refine the final segmentation results. EncNet [53], DANet [17], EMANet [28], and CCNet [25] all utilize different kinds of self-attention mechanisms. EncNet does not have performance gain compared to FCN. In contrast, DANet, EMANet, and CCNet based on the spatial self-attention mechanism all obtain superior performance than FCN. DANet outperforms FCN by more than 0.6% mIoU scores and nearly 1% iIoU scores on both two sets. We analyze that EncNet utilizes the channel-wise self-attention mechanism to build the global context, which cannot preserve the local details well, especially for the high-hanging scenes that contain different sizes of traffic participants.

Transformer structure has been successfully applied to the computer vision tasks [3, 15], which often achieves better recognition results than the convolutional neural network structure. The typical transformer structure stacks

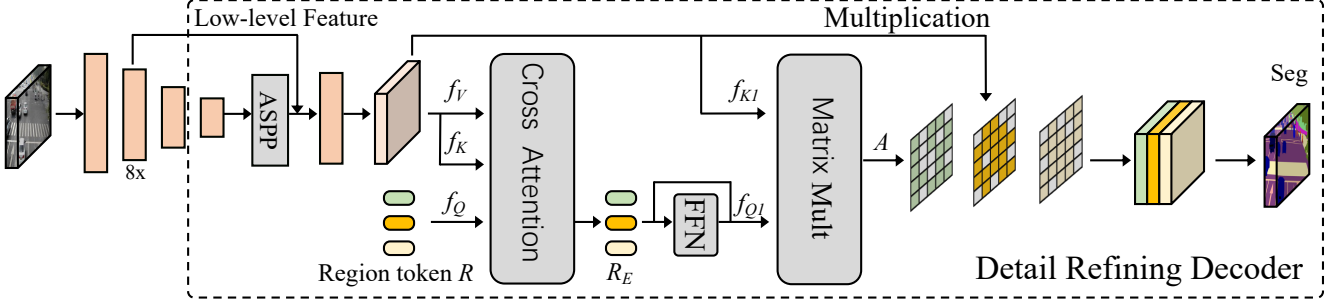


Figure 5. Pipeline of the detail refining decoder. Our decoder contains two parts. The first part is similar to the decoder presented in DeeplabV3+ [7]. Differently, we use the feature maps from the third stage ($\times 8$ downsampling compared to the input) to the feature maps from ASPP. The second part is the proposed region refining module.

several encoder blocks that first utilize the residual self-attention network, followed by the feedforward neural network. SETR [60], Segformer [45], Swin-UperNet [33], and SegNeXt [20] all utilize the transformer structure as the backbone for scene parsing. Among them, SETR achieves much worse parsing results, while other transformer structures obtain superior results than the convolutional backbone. Although Segformer-B2 [45] achieves higher mIoU scores than FCN by about 1.3 %, its iIoU score is even lower than FCN. Among them, UperNet [44] using Swin [33] backbone performs much better than the ResNet50 [22] backbone in terms of both the mIoU and iIoU metrics. Besides, compared with Swin-UperNet, SegNeXt obtains a similar performance with only about 20% parameters and 7% GFlops. We observe that the SegNeXt-Large model achieves fewer gains than the SegNeXt-Base model, as shown in Tab. 3. In this paper, we design a more powerful decoder that can improve both the SegNeXt-Base and SegNeXt-Large models.

In summary, the encoder-decoder structure, spatial self-attention mechanism, and transformer structure are very useful strategies for improving the high-hanging scene parsing. In the following, according to the strategies, we will design a more powerful decoder to generate accurate high-hanging scene results.

5. Method

As analyzed in Sec. 3, high-hanging scenes usually capture much more traffic content than the driving scenes and the scale and shape variances of different semantic regions are much larger. Besides, small things and stuff take a large proportion. These situations make accurately parsing the high-hanging scenes difficult. To adapt to the high-hanging scenes, we propose a detail refining decoder. The design principles of our decoder are two-fold.

First, as the output feature maps of the backbone have a small resolution, building decoders based on the low-resolution features usually generates coarse parsing results and hence largely affects the small object parsing. As verified in some previous works [31, 40, 42], the low-level high-

resolution features are helpful for segmenting small objects. Thus, we utilize the encoder-decoder structure to fuse the low-resolution and high-resolution features to improve the small object parsing.

Second, as analyzed in Sec. 4, self-attention is an efficient way to encode spatial information for the high-hanging scene parsing. However, directly applying the self-attention mechanism to encode high-resolution features will consume huge computation resources especially when processing high-resolution traffic scene images. Inspired by [9] that learns representations for each segment region, we propose to introduce several region tokens and build pairwise correlations between each region token and each patch tokens from the high-resolution features.

5.1. Overall Pipeline

We construct the scene parsing network for high-hanging scenes based on the valuable tips summarized in Sec. 4. First, we adopt the powerful encoder presented in SegNeXt [20] as our encoder, which achieves good results with low computational costs on our TSP6K dataset. Then, we build a detail refining decoder (DRD) upon the encoder to generate high-hanging scene parsing results. The pipeline of the detail refining decoder is shown in Fig. 5, which contains two parts: For the first part, we follow the decoder design of DeepLabv3+ [7] to generate fine-level feature maps. Note that we do not use the $\times 4$ downsampling features from the second stage but the $\times 8$ ones from the third stage as suggested by [20]. The ASPP module is added upon the encoder directly. The second part is the region refining module, which is described in the following subsection.

5.2. Region Refining Module

The region refining module is proposed to refine different semantic regions in the traffic image. Formally, let $F \in \mathbb{R}^{H \times W \times C}$ denote the flattened features from the first part of the decoder, where H , W , and C denote the height, width, and number of channels, respectively. Let $R \in \mathbb{R}^{N \times C}$ denote N learnable region tokens, each of which is a C -dimensional vector. The flattened features F

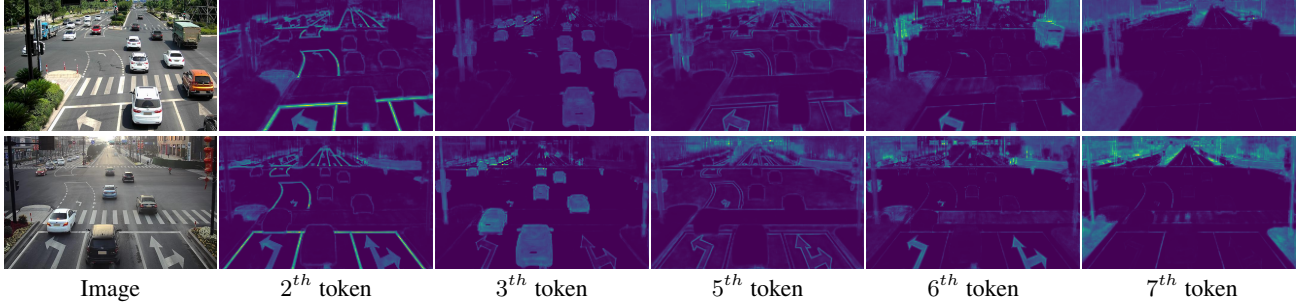


Figure 6. Visualizations of the attention map corresponding to each token. We randomly select several tokens for visualization. One can see that the visualizations associated with different region tokens focus on different semantic regions. These region tokens can help our method better process the region details.

and the learnable region tokens R are separately sent into three linear layers to generate the query, key, and value as follows:

$$R_Q, F_K, F_V = f_Q(R), f_K(F), f_V(F), \quad (1)$$

where $f_Q(R)$, $f_K(F)$, and $f_V(F)$ are linear layers and $R_Q \in \mathbb{R}^{N \times C}$, $F_K \in \mathbb{R}^{HW \times C}$, $F_V \in \mathbb{R}^{HW \times C}$. We compute the multi-head cross-attention between F and R as follows:

$$R_E = \text{Softmax} \left(\frac{R_Q F_K^T}{\sqrt{C}} \right) F_V + R, \quad (2)$$

where $R_E \in \mathbb{R}^{N \times C}$ is the resulting region embeddings. The region embeddings are then sent into a feed-forward network, which is formulated as:

$$R_O = \text{FFN}(R_E) + R_E, \quad (3)$$

where R_O is the output of the feed-forward network. Here, following [41], only the region tokens R_E are sent to the feed-forward block for an efficient process.

Next, R_O and F are delivered to two linear layers to generate a group of new query and key as follows:

$$R_{Q1}, F_{K1} = f_{Q1}(R_O), f_{K1}(F). \quad (4)$$

We perform the matrix multiplication between R_{Q1} and F_{K1} to produce attention maps by

$$A = \text{Softmax} \left(\frac{R_{Q1} F_{K1}^T}{\sqrt{C}} \right), \quad (5)$$

where $A \in \mathbb{R}^{N \times HW}$ denotes N attention maps and each attention map is associated with a semantic region. When we attain the region attention maps, we combine A and $F \in \mathbb{R}^{HW \times C}$ via broadcast multiplications, which can be written as follows:

$$S_{i,j,k} = A_{i,j} \cdot F_{j,k}, \quad (6)$$

where $S \in \mathbb{R}^{N \times HW \times C}$ is the output. Finally, S is permuted and reshaped and sent into a class-wise convolutional layer to generate the final segmentation maps. In the following, we will show the effectiveness of the proposed segmentation network in the experiment section.

Table 4. Ablation study on the selection of the number of tokens and attention heads.

Settings	#Tokens	Attention Heads	mIoU _{val}	iIoU _{val}
1	1	12	75.0	56.9
2	10	12	75.4	58.1 _(+1.2)
3	20	12	75.4	58.3 _(+1.4)
4	20	24	75.4	58.2 _(+1.3)

6. Experiments

To verify the effectiveness of the proposed detail refining decoder, we conduct several ablation experiments on the number of region tokens, and attention heads. Besides, we also compare our method with the previous state-of-the-art methods on the proposed dataset. Experiment details can be found in our supplementary materials.

6.1. Ablation Study

The number of region tokens and heads. First, we study the impact of the number of tokens and heads on the performance. As shown in Tab. 4, using 10 region tokens instead of 1 region token brings 0.4% mIoU scores and 1.2% iIoU scores improvement. This fact demonstrates that the number of region tokens largely affects the parsing of traffic participants, especially for small objects. When further improving the number of region tokens, we observe little performance gain, which indicates 10 tokens are enough for semantic region refining. Besides, we also attempt to increase the number of attention heads. It can be seen that adding more heads brings no performance gain.

For readers to better understand the region tokens, we have visualized the attention maps of different tokens, as shown in Fig. 6. It can be seen that different tokens are responsible for different semantic regions.

Region tokens vs. Class Tokens. In the design of the detail refining decoder, we utilize the region tokens to refine a specific semantic region. Here, one may raise a question: “How would the performance go when we utilize class to-

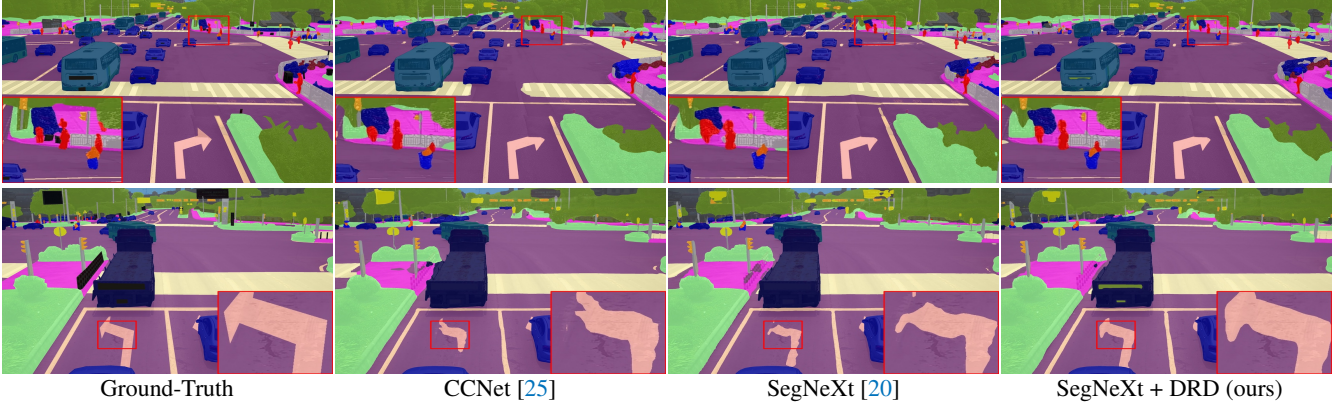


Figure 7. Visualization of the scene parsing results from different methods. One can see that our method can well process the region details. When taking the bottom scene as an example, our method can generate a more accurate mask for the arrow while other methods fail. Zoom in for the best view.

kens as done the original Transformers instead of the region tokens”? We perform an experiment that learns 21 class tokens, each of which corresponds to a class. The final concatenated features are sent to a depth-wise convolutional layer with 21 groups. When using the class tokens, we can obtain 75.3% mIoU scores and 57.1% iIoU scores on the validation set. Compared with the using of class tokens, the decoder with 10 region tokens can obtain 58.1% iIoU scores, which works better than using class tokens. Besides, when the number of classes in the dataset is large, the class tokens will consume high computational costs. In contrast, using the region tokens is more flexible in that there is no need to adjust the number of region tokens when the number of classes rises.

The importance of the encoder-decoder structure. In Sec. 4.1, we have analyzed that the encoder-decoder structure is important for small object parsing. Thus, we apply the encoder-decoder structure to our segmentation network. Without the encoder-decoder structure, i.e., we directly connect the region refining module to the encoder, the mIoU score decreases by 0.2%. The iIoU score decreases by 0.8%. This experiment indicates that the high-resolution low-level features can benefit the parsing of the traffic participants. Thus, the encoder-decoder structure is important for high-hanging scene parsing.

6.2. Comparisons with SOTA

After performing a sanity check for the detail refining decoder, we compare the result of the proposed method with other methods on the TSP6K dataset. Tab. 3 lists the performance of different methods. It can be seen that our method outperforms all previous methods and achieves the best results in terms of both the two metrics. Besides, the original Hamburger decoder [19] cannot further improve the performance of the SegNeXt-Large model. However, when replacing the Hamburger decoder with the proposed detail re-

fining decoder, the performance is largely improved, outperforming the Hamburger decoder by 1.3% mIoU scores and 1.3% nIoU scores on the validation set. The evaluation results demonstrate the effectiveness of the proposed decoder in parsing the high-hanging scenes. Furthermore, we provide some qualitative results in Fig. 7 for visual comparison. We can see that our method is more suitable for processing the region details than CCNet and SegNeXt.

7. Limitations

In this paper, based on the TSP6K dataset, we have evaluated a series of previous popular scene parsing methods. However, we do not explore the scene panoptic segmentation and instance segmentation though instance annotations are also provided. We hope the proposed dataset can encourage the community to develop more powerful scene parsing methods, instance segmentation methods, and panoptic scene parsing methods for high-hanging scenes.

8. Conclusions

In this paper, we have constructed the TSP6K dataset, focusing on the high-hanging traffic scenes. We have provided each traffic image with a semantic and instance label. Based on the finely annotated the TSP6K dataset, we have evaluated the previous popular scene parsing methods and summarized some useful tips. To improve the performance of the high-hanging scene parsing, we design a detail refining decoder, which utilizes the high-resolution features from the encoder-decoder structure and refines different semantic regions based on the self-attention mechanism. The detail refining decoder learns several region tokens and computes attention maps for different semantic regions. The attention maps are used to refine the pixel affinity in different semantic regions. Experiments have shown the effectiveness of the proposed detail refining decoder.

References

- [1] Vijay Badrinarayanan, Alex Kendall, and Roberto Cipolla. Segnet: A deep convolutional encoder-decoder architecture for image segmentation. *IEEE Trans. Pattern Anal. Mach. Intell.*, 39(12):2481–2495, 2017.
- [2] Holger Caesar, Jasper Uijlings, and Vittorio Ferrari. Coco-stuff: Thing and stuff classes in context. In *IEEE Conf. Comput. Vis. Pattern Recog.*, pages 1209–1218, 2018.
- [3] Nicolas Carion, Francisco Massa, Gabriel Synnaeve, Nicolas Usunier, Alexander Kirillov, and Sergey Zagoruyko. End-to-end object detection with transformers. In *Eur. Conf. Comput. Vis.*, pages 213–229. Springer, 2020.
- [4] Liang-Chieh Chen, George Papandreou, Iasonas Kokkinos, Kevin Murphy, and Alan L Yuille. Semantic image segmentation with deep convolutional nets and fully connected crfs. In *Int. Conf. Learn. Represent.*, 2015.
- [5] Liang-Chieh Chen, George Papandreou, Iasonas Kokkinos, Kevin Murphy, and Alan L Yuille. Deeplab: Semantic image segmentation with deep convolutional nets, atrous convolution, and fully connected crfs. *IEEE Trans. Pattern Anal. Mach. Intell.*, 40(4):834–848, 2017.
- [6] Liang-Chieh Chen, George Papandreou, Florian Schroff, and Hartwig Adam. Rethinking atrous convolution for semantic image segmentation. *arXiv preprint arXiv:1706.05587*, 2017.
- [7] Liang-Chieh Chen, Yukun Zhu, George Papandreou, Florian Schroff, and Hartwig Adam. Encoder-decoder with atrous separable convolution for semantic image segmentation. In *Eur. Conf. Comput. Vis.*, pages 801–818, 2018.
- [8] Bowen Cheng, Liang-Chieh Chen, Yunchao Wei, Yukun Zhu, Zilong Huang, Jinjun Xiong, Thomas S Huang, Wen-Mei Hwu, and Honghui Shi. Spgnet: Semantic prediction guidance for scene parsing. In *Int. Conf. Comput. Vis.*, pages 5218–5228, 2019.
- [9] Bowen Cheng, Ishan Misra, Alexander G Schwing, Alexander Kirillov, and Rohit Girdhar. Masked-attention mask transformer for universal image segmentation. In *IEEE Conf. Comput. Vis. Pattern Recog.*, pages 1290–1299, 2022.
- [10] Bowen Cheng, Alex Schwing, and Alexander Kirillov. Per-pixel classification is not all you need for semantic segmentation. *Adv. Neural Inform. Process. Syst.*, 34:17864–17875, 2021.
- [11] MMSegmentation Contributors. MMSegmentation: Openmmlab semantic segmentation toolbox and benchmark. <https://github.com/open-mmlab/mms Segmentation>, 2020.
- [12] Marius Cordts, Mohamed Omran, Sebastian Ramos, Timo Rehfeld, Markus Enzweiler, Rodrigo Benenson, Uwe Franke, Stefan Roth, and Bernt Schiele. The cityscapes dataset for semantic urban scene understanding. In *IEEE Conf. Comput. Vis. Pattern Recog.*, pages 3213–3223, 2016.
- [13] Jonathan Cresspo, Jose Carlos Castillo, Oscar Martinez Mozos, and Ramon Barber. Semantic information for robot navigation: A survey. *Applied Sciences*, 10(2):497, 2020.
- [14] Dengxin Dai and Luc Van Gool. Dark model adaptation: Semantic image segmentation from daytime to nighttime. In *2018 21st International Conference on Intelligent Transportation Systems (ITSC)*, pages 3819–3824. IEEE, 2018.
- [15] Alexey Dosovitskiy, Lucas Beyer, Alexander Kolesnikov, Dirk Weissenborn, Xiaohua Zhai, Thomas Unterthiner, Mostafa Dehghani, Matthias Minderer, Georg Heigold, Sylvain Gelly, et al. An image is worth 16x16 words: Transformers for image recognition at scale. In *Int. Conf. Learn. Represent.*, 2021.
- [16] Mark Everingham, SM Ali Eslami, Luc Van Gool, Christopher KI Williams, John Winn, and Andrew Zisserman. The pascal visual object classes challenge: A retrospective. *Int. J. Comput. Vis.*, 111(1):98–136, 2015.
- [17] Jun Fu, Jing Liu, Haijie Tian, Yong Li, Yongjun Bao, Zhiwei Fang, and Hanqing Lu. Dual attention network for scene segmentation. In *IEEE Conf. Comput. Vis. Pattern Recog.*, pages 3146–3154, 2019.
- [18] Andreas Geiger, Philip Lenz, Christoph Stiller, and Raquel Urtasun. Vision meets robotics: The kitti dataset. *The International Journal of Robotics Research*, 32(11):1231–1237, 2013.
- [19] Zhengyang Geng, Meng-Hao Guo, Hongxu Chen, Xia Li, Ke Wei, and Zhouchen Lin. Is attention better than matrix decomposition? In *Int. Conf. Learn. Represent.*, 2021.
- [20] Meng-Hao Guo, Cheng-Ze Lu, Qibin Hou, Zhengning Liu, Ming-Ming Cheng, and Shi-Min Hu. Segnext: Rethinking convolutional attention design for semantic segmentation. In *Adv. Neural Inform. Process. Syst.*, 2022.
- [21] Junjun He, Zhongying Deng, Lei Zhou, Yali Wang, and Yu Qiao. Adaptive pyramid context network for semantic segmentation. In *IEEE Conf. Comput. Vis. Pattern Recog.*, pages 7519–7528, 2019.
- [22] Kaiming He, Xiangyu Zhang, Shaoqing Ren, and Jian Sun. Deep residual learning for image recognition. In *IEEE Conf. Comput. Vis. Pattern Recog.*, pages 770–778, 2016.
- [23] Qibin Hou, Li Zhang, Ming-Ming Cheng, and Jiashi Feng. Strip pooling: Rethinking spatial pooling for scene parsing. In *IEEE Conf. Comput. Vis. Pattern Recog.*, pages 4003–4012, 2020.
- [24] Xinyu Huang, Peng Wang, Xinjing Cheng, Dingfu Zhou, Qichuan Geng, and Ruigang Yang. The apolloscape open dataset for autonomous driving and its application. *IEEE Trans. Pattern Anal. Mach. Intell.*, 42(10):2702–2719, 2019.
- [25] Zilong Huang, Xinggang Wang, Lichao Huang, Chang Huang, Yunchao Wei, and Wenyu Liu. Ccnet: Criss-cross attention for semantic segmentation. In *Int. Conf. Comput. Vis.*, pages 603–612, 2019.
- [26] Galadrielle Humblot-Renaux, Letizia Marchegiani, Thomas B Moeslund, and Rikke Gade. Navigation-oriented scene understanding for robotic autonomy: Learning to segment driveability in egocentric images. *IEEE Robotics and Automation Letters*, 7(2):2913–2920, 2022.
- [27] Xiaojie Jin, Huaxin Xiao, Xiaohui Shen, Jimei Yang, Zhe Lin, Yunpeng Chen, Zequn Jie, Jiashi Feng, and Shuicheng Yan. Predicting scene parsing and motion dynamics in the future. In *Adv. Neural Inform. Process. Syst.*, volume 30, 2017.

- [28] Xia Li, Zhisheng Zhong, Jianlong Wu, Yibo Yang, Zhouchen Lin, and Hong Liu. Expectation-maximization attention networks for semantic segmentation. In *Int. Conf. Comput. Vis.*, pages 9167–9176, 2019.
- [29] Xiaodan Liang, Hongfei Zhou, and Eric Xing. Dynamic-structured semantic propagation network. In *IEEE Conf. Comput. Vis. Pattern Recog.*, pages 752–761, 2018.
- [30] Guosheng Lin, Anton Milan, Chunhua Shen, and Ian Reid. Refinenet: Multi-path refinement networks for high-resolution semantic segmentation. In *IEEE Conf. Comput. Vis. Pattern Recog.*, pages 1925–1934, 2017.
- [31] Tsung-Yi Lin, Piotr Dollár, Ross Girshick, Kaiming He, Bharath Hariharan, and Serge Belongie. Feature pyramid networks for object detection. In *IEEE Conf. Comput. Vis. Pattern Recog.*, pages 2117–2125, 2017.
- [32] Tsung-Yi Lin, Michael Maire, Serge Belongie, James Hays, Pietro Perona, Deva Ramanan, Piotr Dollár, and C Lawrence Zitnick. Microsoft coco: Common objects in context. In *Eur. Conf. Comput. Vis.*, 2014.
- [33] Ze Liu, Yutong Lin, Yue Cao, Han Hu, Yixuan Wei, Zheng Zhang, Stephen Lin, and Baining Guo. Swin transformer: Hierarchical vision transformer using shifted windows. In *Int. Conf. Comput. Vis.*, pages 10012–10022, 2021.
- [34] Jonathan Long, Evan Shelhamer, and Trevor Darrell. Fully convolutional networks for semantic segmentation. In *IEEE Conf. Comput. Vis. Pattern Recog.*, pages 3431–3440, 2015.
- [35] Yisheng Lv, Yanjie Duan, Wenwen Kang, Zhengxi Li, and Fei-Yue Wang. Traffic flow prediction with big data: a deep learning approach. *IEEE Transactions on Intelligent Transportation Systems*, 16(2):865–873, 2014.
- [36] Gerhard Neuhold, Tobias Ollmann, Samuel Rota Bulo, and Peter Kotschieder. The mapillary vistas dataset for semantic understanding of street scenes. In *Int. Conf. Comput. Vis.*, pages 4990–4999, 2017.
- [37] Olaf Ronneberger, Philipp Fischer, and Thomas Brox. U-net: Convolutional networks for biomedical image segmentation. In *International Conference on Medical image computing and computer-assisted intervention*, pages 234–241. Springer, 2015.
- [38] Christos Sakaridis, Dengxin Dai, and Luc Van Gool. Guided curriculum model adaptation and uncertainty-aware evaluation for semantic nighttime image segmentation. In *Int. Conf. Comput. Vis.*, pages 7374–7383, 2019.
- [39] Robin Strudel, Ricardo Garcia, Ivan Laptev, and Cordelia Schmid. Segmenter: Transformer for semantic segmentation. In *Int. Conf. Comput. Vis.*, pages 7262–7272, 2021.
- [40] Zhi Tian, Chunhua Shen, and Hao Chen. Conditional convolutions for instance segmentation. In *Eur. Conf. Comput. Vis.*, pages 282–298. Springer, 2020.
- [41] Hugo Touvron, Matthieu Cord, Alexandre Sablayrolles, Gabriel Synnaeve, and Hervé Jégou. Going deeper with image transformers. In *Int. Conf. Comput. Vis.*, pages 32–42, 2021.
- [42] Xinlong Wang, Tao Kong, Chunhua Shen, Yuning Jiang, and Lei Li. Solo: Segmenting objects by locations. In *Eur. Conf. Comput. Vis.*, pages 649–665. Springer, 2020.
- [43] Huikai Wu, Junge Zhang, Kaiqi Huang, Kongming Liang, and Yu Yizhou. Fastfcn: Rethinking dilated convolution in the backbone for semantic segmentation. In *arXiv preprint arXiv:1903.11816*, 2019.
- [44] Tete Xiao, Yingcheng Liu, Bolei Zhou, Yuning Jiang, and Jian Sun. Unified perceptual parsing for scene understanding. In *Eur. Conf. Comput. Vis.*, pages 418–434, 2018.
- [45] Enze Xie, Wenhai Wang, Zhiding Yu, Anima Anandkumar, Jose M Alvarez, and Ping Luo. Segformer: Simple and efficient design for semantic segmentation with transformers. *Adv. Neural Inform. Process. Syst.*, 34:12077–12090, 2021.
- [46] Changqian Yu, Changxin Gao, Jingbo Wang, Gang Yu, Chunhua Shen, and Nong Sang. Bisenet v2: Bilateral network with guided aggregation for real-time semantic segmentation. *Int. J. Comput. Vis.*, pages 1–18, 2021.
- [47] Changqian Yu, Jingbo Wang, Chao Peng, Changxin Gao, Gang Yu, and Nong Sang. Bisenet: Bilateral segmentation network for real-time semantic segmentation. In *Eur. Conf. Comput. Vis.*, pages 325–341, 2018.
- [48] Fisher Yu, Haofeng Chen, Xin Wang, Wenqi Xian, Yingying Chen, Fangchen Liu, Vashisht Madhavan, and Trevor Darrell. Bdd100k: A diverse driving dataset for heterogeneous multitask learning. In *IEEE Conf. Comput. Vis. Pattern Recog.*, pages 2636–2645, 2020.
- [49] Yuhui Yuan, Xilin Chen, and Jingdong Wang. Object-contextual representations for semantic segmentation. 2020.
- [50] Yuhui Yuan, Lang Huang, Jianyuan Guo, Chao Zhang, Xilin Chen, and Jingdong Wang. Ocnet: Object context for semantic segmentation. *Int. J. Comput. Vis.*, 129(8):2375–2398, 2021.
- [51] Oliver Zendel, Katrin Honauer, Markus Murschitz, Daniel Steininger, and Gustavo Fernandez Dominguez. Wilddash-creating hazard-aware benchmarks. In *Eur. Conf. Comput. Vis.*, pages 402–416, 2018.
- [52] Oliver Zendel, Matthias Schörghuber, Bernhard Rainer, Markus Murschitz, and Csaba Belezna. Unifying panoptic segmentation for autonomous driving. In *IEEE Conf. Comput. Vis. Pattern Recog.*, pages 21351–21360, 2022.
- [53] Hang Zhang, Kristin Dana, Jianping Shi, Zhongyue Zhang, Xiaogang Wang, Amrith Tyagi, and Amit Agrawal. Context encoding for semantic segmentation. In *IEEE Conf. Comput. Vis. Pattern Recog.*, pages 7151–7160, 2018.
- [54] Rui Zhang, Sheng Tang, Yongdong Zhang, Jintao Li, and Shuicheng Yan. Scale-adaptive convolutions for scene parsing. In *Int. Conf. Comput. Vis.*, pages 2031–2039, 2017.
- [55] Wenqiang Zhang, Zilong Huang, Guozhong Luo, Tao Chen, Xinggang Wang, Wenyu Liu, Gang Yu, and Chunhua Shen. Topformer: Token pyramid transformer for mobile semantic segmentation. In *IEEE Conf. Comput. Vis. Pattern Recog.*, pages 12083–12093, 2022.
- [56] Wenwei Zhang, Jiangmiao Pang, Kai Chen, and Chen Change Loy. K-net: Towards unified image segmentation. In *Adv. Neural Inform. Process. Syst.*, volume 34, pages 10326–10338, 2021.
- [57] Hengshuang Zhao, Xiaojuan Qi, Xiaoyong Shen, Jianping Shi, and Jiaya Jia. Icnet for real-time semantic segmentation on high-resolution images. In *Eur. Conf. Comput. Vis.*, pages 405–420, 2018.

- [58] Hengshuang Zhao, Jianping Shi, Xiaojuan Qi, Xiaogang Wang, and Jiaya Jia. Pyramid scene parsing network. In *IEEE Conf. Comput. Vis. Pattern Recog.*, pages 2881–2890, 2017.
- [59] Hengshuang Zhao, Yi Zhang, Shu Liu, Jianping Shi, Chen Change Loy, Dahua Lin, and Jiaya Jia. Psanet: Point-wise spatial attention network for scene parsing. In *Eur. Conf. Comput. Vis.*, pages 267–283, 2018.
- [60] Sixiao Zheng, Jiachen Lu, Hengshuang Zhao, Xiatian Zhu, Zekun Luo, Yabiao Wang, Yanwei Fu, Jianfeng Feng, Tao Xiang, Philip HS Torr, et al. Rethinking semantic segmentation from a sequence-to-sequence perspective with transformers. In *IEEE Conf. Comput. Vis. Pattern Recog.*, pages 6881–6890, 2021.
- [61] Bolei Zhou, Hang Zhao, Xavier Puig, Sanja Fidler, Adela Barriuso, and Antonio Torralba. Scene parsing through ade20k dataset. In *IEEE Conf. Comput. Vis. Pattern Recog.*, pages 633–641, 2017.
- [62] Zhen Zhu, Mengde Xu, Song Bai, Tengpeng Huang, and Xiang Bai. Asymmetric non-local neural networks for semantic segmentation. In *Int. Conf. Comput. Vis.*, pages 593–602, 2019.